Two-Dimensional Melting of Two- and Three-Component Mixtures

Yan-Wei Li* and Yugui Yao†
Key Laboratory of Advanced Optoelectronic Quantum Architecture and Measurement (MOE), School of Physics, Beijing Institute of Technology, Beijing 100081, China

Massimo Pica Ciamarra‡
Division of Physics and Applied Physics, School of Physical and Mathematical Sciences, Nanyang Technological University, Singapore 637371, Singapore;
CNR–SPIN, Dipartimento di Scienze Fisiche, Università di Napoli Federico II, I-80126 Napoli, Italy;
and CNRS@CREATE LTD, 1 Create Way, #08-01 CREATE Tower, Singapore 138602, Singapore

(Received 27 February 2023; revised 16 May 2023; accepted 1 June 2023; published 22 June 2023)

We elucidate the interplay between diverse two-dimensional melting pathways and establish solid-hexatic and hexatic-liquid transition criteria via the numerical simulations of the melting transition of two- and three-component mixtures of hard polygons and disks. We show that a mixture's melting pathway may differ from its components and demonstrate eutectic mixtures that crystallize at a higher density than their pure components. Comparing the melting scenario of many two- and three-component mixtures, we establish universal melting criteria: the solid and hexatic phases become unstable as the density of topological defects, respectively, overcomes $\rho_{d,s} \simeq 0.046$ and $\rho_{d,h} \simeq 0.123$.

DOI: 10.1103/PhysRevLett.130.258202

The nature of the melting of two-dimensional (2D) solids is a long-standing and fascinating problem in statistical physics [1–16]. According to the Kosterlitz-Thouless-Halperin-Nelson-Young (KTHNY) theory [1–3], 2D solids melt via a continuous solid to hexatic transition driven by the unbinding of dislocation pairs, followed by a continuous hexatic to liquid transition driven by the further unbinding of isolated dislocation into disclinations. Two alternative melting scenarios are possible. In the mixed case, the solid-to-hexatic transition is continuous, while the hexatic-to-liquid transition is discontinuous; finally, the solid transforms into a liquid via a first-order transition in the discontinuous case. Recent computational and methodological advances have allowed establishing the melting scenario of pure two-dimensional substances [8–20]. It has been clarified, for instance, that shape controls the melting scenario in hard-particle systems [8–10] with, e.g., hexagons, disks, and pentagons following the KTHNY, mixed and discontinuous melting [10,18]. In soft repulsive systems, the softness of the interparticle interaction influences the melting pathway [17], while attractive interactions promote discontinuous melting [10].

Phase diagrams are more complex in many-component systems. The relative fractions become an essential control variable, novel phases may emerge, and melting may interplay with phase separation. These aspects have been thoroughly investigated in three-dimensional systems but are almost unexplored in two dimensions [21–23]. Can a mixture melt via a scenario different from its components? Is there a eutectic mixture whose melting temperature is lower than its components or, for hard particles, a mixture that melts at a density higher than its components? Do topological defects correlate with the phase behavior as in pure systems [24]? Investigating the melting of mixtures further offers the possibility of validating proposed melting criteria based on a generalization of Lindemann's approach [25–27] or topological defects [22,24].

In this Letter, we investigate the interplay between diverse melting mechanisms by tuning the relative composition of two- and three-component mixtures of hard particles. In hexagons + disks and pentagons + hexagons mixtures, the melting pathway smoothly crossovers from that of a pure substance to that of the other. On the contrary, disks + pentagons mixtures may follow the KTHNY melting scenario, not occurring in pure disks or pentagons. The study of a large catalog of two-dimensional systems further demonstrates that the density of topological defects ρ_d controls the stability of the solid and hexatic phases. As the density decreases, the solid phase becomes unstable at $\rho_{d,s} \simeq 0.046$, and the hexatic one at $\rho_{d,h} \simeq 0.123$ [22]. Our predictions open new routes to self-assembly in two dimensions [28] and can be experimentally verified by changing a mixture's composition.

We construct pentagons, hexagons, and disks with the same circumscribing circle of diameter d, by lumping together $N_d = 40$ or 42 beads equally spaced along the perimeter, as detailed in Supplemental Material (SM) [29] and in [10]. Beads of different particles with separation distance r_b interact via the Weeks,

Chandler, and Andersen (WCA) potential [30]: $V_{\mathrm{WCA}}(r_b) = 4\epsilon[(\sigma/r_b)^{12} - (\sigma/r_b)^6 + c]$ for $r_b \leq r_{\mathrm{cut}} = 2^{1/6}\sigma$. The constant c enforces $V_{\mathrm{WCA}}(r_{\mathrm{cut}}) = 0$. We set $\sigma \simeq 0.14d$. We carry out molecular dynamics simulations in the canonical ensemble, under periodic boundary conditions within a rectangular box with a side length ratio of $2:\sqrt{3}$ to accommodate the triangular lattice, fixing the temperature via the Nosé-Hoover thermostat. We fix $T = 20\epsilon/k_b$ if not otherwise specified and demonstrate in Fig. S4 [29] that the choice of the temperature values has no effect on the melting scenario. All simulations are performed using the graphics processing unit-accelerated GALAMOST package [31]. We ensure thermal equilibration as detailed in Fig. S2 [29], and report results for systems of $N = 20\,521$ particles, where finite size effects are negligible as detailed in Fig. S3 [29].

Most previous investigations of the equilibrium phase diagram of two-dimensional mixtures of particles interacting via purely repulsive forces considered the specific case of hard disks. These studies focused on identifying the many possible crystalline phases determined by the size ratio and the relative fraction, e.g., [32–35], and on the stability of the hard-disk melting scenario [21–23]. In these systems, geometric frustration stemming from the size disparity prevents the triangular lattice from being the ground state. We depart from these previous works as we consider mixtures of particles with similar sizes but different shapes. By focusing on mixtures of particles with similar sizes, all crystallizing in the triangular lattice with the same lattice constant, we avoid phase separation [36], glass formation [37], and the emergence of complex crystalline phases on increasing the density. Yet, the shapes we consider melt via different pathways. Hence, while previous works considered the competition between different possible ground states, we explore the competition between alternative crystallization pathways to the same ground state.

To determine the melting scenario, we first consider if the isothermal equation of state (EOS) possesses a Mayer-Wood loop indicating the presence of a first-order transition [38]. If so, we fit the EOS to a fifth-order polynomial to identify the coexistence boundaries and further investigate the local density distribution in the coexisting region [39]. Outside the coexistence region, or in its absence, we determine the pure phases by investigating the correlation functions $c(r)$ and $g_6(r)$ of the translational and bond-orientational order [1,8,40]. In the liquid phase, both functions decay exponentially. In the hexatic phase [1], the system possesses quasi-long-range bond-orientational order and short-range translational order, so that $g_6(r) \propto r^{-\eta_6}$ with $\eta_6 < 1/4$, while $c(r)$ decays exponentially. In the solid phase, $g_6(r)$ does not decay as the bond-orientational order is extended, while $c(r) \propto r^{-\eta}$ with $\eta \leq 1/3$ decay algebraically as Mermin-Wagner fluctuations makes the translational order quasi-long-ranged [41].

Figure 1 illustrates the dependence of the melting scenario of disks + pentagons mixtures on the fraction of disks, f_d. The equation of state (a) reveals a first-order transition at both small and large f_d that corresponds to the discontinuous solid-liquid transition of pure pentagons and the discontinuous liquid-hexatic transitions of pure disks. When the transition is discontinuous, the local density distribution for state points inside the coexistence region [panel (b)] shows clear bimodality. Consistently with the absence of segregation phenomena, the coexisting phases have the same disk fraction f_d.

The translational and bond-orientational correlation functions illustrated in Figs. 1(c) and 1(d) clarify that on

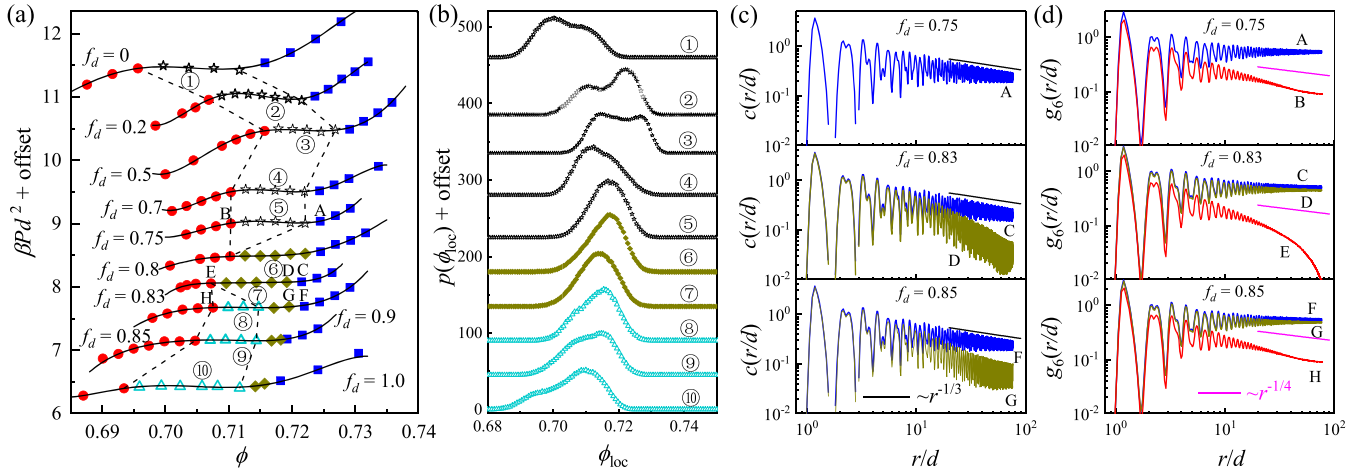

FIG. 1. Melting of disks + pentagons mixtures. (a) Isothermal equation of state. Data are vertically shifted for clarity, and the fraction of disks increases from top to bottom. (b) Probability distribution of the local density, and (c) the translational and (d) the bond-orientational correlation functions for selected state points marked in (a). Symbols and colors identify different phases: liquid (solid red circles); hexatic (olive diamonds); solid (solid blue squares); liquid-solid coexistence (open stars); liquid-hexatic coexistence (open cyan triangles).

increasing the disk fraction, the discontinuous hard-pentagons melting scenario first transforms into the continuous KTHNY scenario and then into that of hard disk. Indeed, we find melting is continuous for disk fractions around $f_d \simeq 0.82$. This result demonstrates that a two-component mixture may melt via a scenario different from its components. We notice that the crossover from a mixed to discontinuous melting may not involve an intermediate KTHNY melting scenario, as observed in attractive hard disks [10] as the temperature decreases.

We have also investigated the melting scenario of hexagons + disks and pentagons + hexagons mixtures and provide details in the SM [29]. We summarize our investigations in Fig. 2 by illustrating how the melting scenario of hexagons + disks, disks + pentagons, and pentagons + hexagons varies with the fraction of disks, f_d, and that of hexagons, f_h. The three diagrams match at their boundaries corresponding to the melting behavior of pure disks, pure pentagons, and pure hexagons, which we find to follow the mixed, discontinuous, and KTHNY scenario, consistently with previous results [8,10,18].

Hexagons + disks mixtures [panel (a), left] crossover from the KTHNY to the mixed scenario as the fraction of disks overcomes $f_d \simeq 0.5$, an intermediate value suggesting that these two shapes do not frustrate each other considerably. Conversely, pentagons + hexagons mixtures [panel (a), right] crossover from the discontinuous to the KTHNY scenario as the fraction of hexagons overcomes $f_h \simeq 0.9$: adding a small fraction of pentagons disrupts hexagons' KTHNY melting scenario. Similarly, a small amount of pentagons disrupts the melting scenario of hard disks [panel (a), middle]. However, in this case, on increasing the pentagons fraction, the melting scenario first becomes of KTHNY type and then becomes discontinuous, as we previously noticed.

In hexagons + disks and pentagons + hexagons mixtures, the stability limit $\phi_L(f)$ of the liquid phase weakly depends on f. Conversely, in disks + pentagons mixtures, for $f \simeq 0.5$, the liquid phase is stable up to $\phi_L \simeq 0.715$, a value sensibly higher than that characterizing the pure phases, $\phi_L \simeq 0.70$. This mixture is thus one of the few known examples of eutectic two-dimensional colloidal systems [42].

Melting in two dimensions has historically been related to the evolution of the density of topological defects, clusters of particles not having six neighbors. In the KTHNY scenario [1–3], melting occurs through a continuous solid-hexatic transition driven by the unbinding of dislocation pairs (clusters of four particles with $5+7+5+7$ neighbors), followed by a continuous hexatic-liquid one driven by the further unbinding of isolated dislocation $(5+7)$ into disclinations (5 or 7). While the observation of extended clusters of defective particles [24] suggests a rather complex relation between phase behavior and defects, Guo *et al.* [22] have found that in systems following the KTHNY scenario, at the hexatic-liquid boundary, the density of defective particles acquires a universal value, $\rho_{d,h} = 0.12$. This number then acts as an upper bound for the defects' density in the hexatic phase.

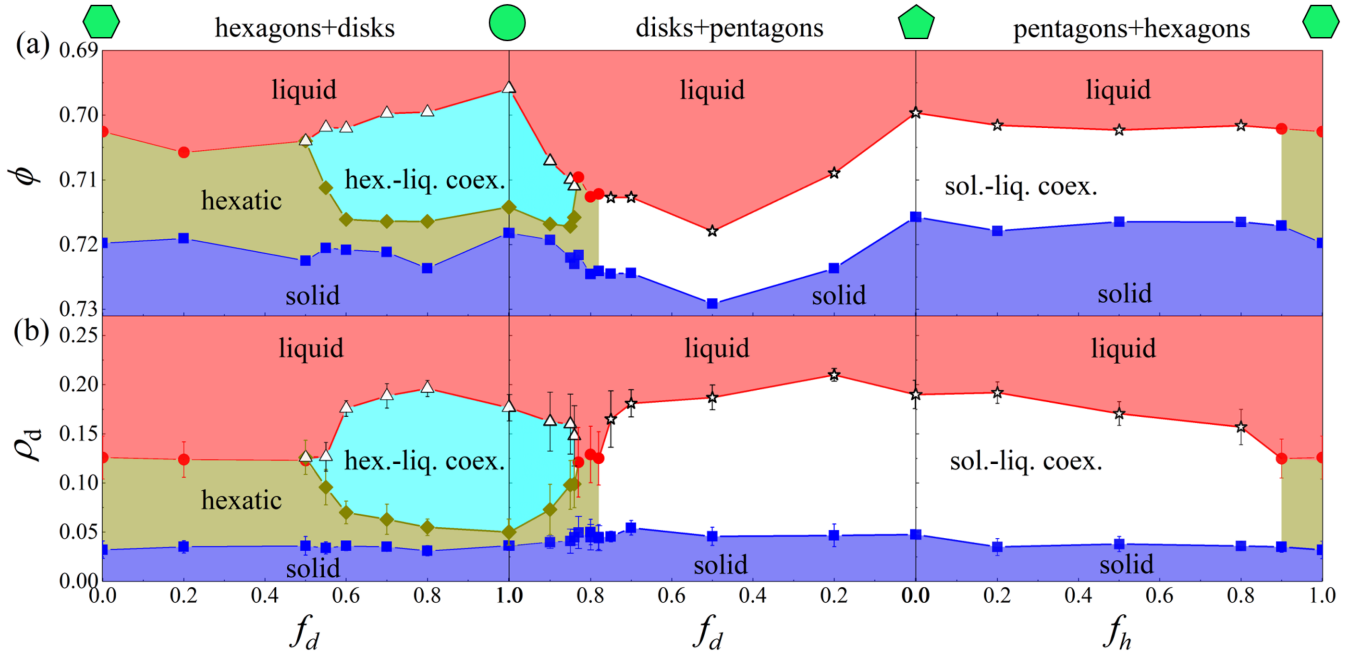

FIG. 2. (a) Phase diagram of hexagons + disks, disks + pentagons, and pentagons + hexagons mixtures, in the relative fraction f and area fraction ϕ plane. (b) the same diagrams are illustrated in the f-ρ_d plane, with ρ_d the density of defective particles that do not have six immediate neighbors. We evaluate ρ_d in 8 subblocks of the system to estimate its error. The liquid-hexatic, solid-hexatic, and solid-coexistence boundaries occur at approximately constant defect densities.

We explore the relationship between defects' density and phase behavior by investigating the phase diagrams in the $\rho_d - f$ plane in Fig. 2(b). We find that the defects' density at the hexatic-liquid boundary (red circles) attains the universal value of $\rho_{d,h} = 0.123 \pm 0.006$, in agreement with the earlier speculation [22]. In addition, we also find the defects' density equals $\rho_{d,s} = 0.046 \pm 0.005$ at the solid-hexatic and solid-coexistence boundaries.

To test the universality of these findings, we examine ternary mixtures of pentagons, hexagons, and disks. For each composition, we investigate the phase behavior as a function of the volume fraction to determine the melting scenario [29]. The ternary phase diagram of Fig. 3(a) summarizes the result of this investigation. Each point in the diagram represents the melting scenario observed at a given composition f_d, f_p, f_h. A point's composition is read by connecting it to the triangle's sides, as illustrated with point "A" for which $f_d = 0.50$, $f_p = 0.25$, and $f_h = 0.25$. Hence, the three corners correspond to the three pure systems and the three sides to the three binary diagrams, e.g., the bottom left corner corresponds to pure pentagons and the "pentagon" side to the disks + pentagons mixture.

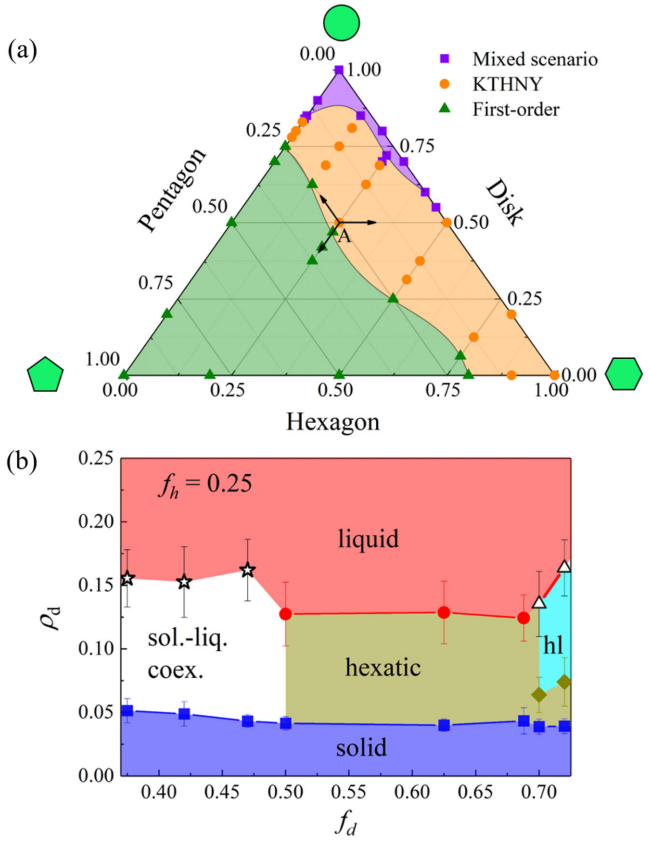

FIG. 3. (a) Ternary phase diagram for mixtures of pentagons, hexagons, and disks. Each point within the triangle corresponds to a composition determined by the intersections of lines passing through that point and the sides of the triangle. For example, in point A, the fraction of disks, pentagons, and hexagons are 0.50, 0.25, and 0.25. (b) Phase diagram at fixed hexagon fraction $f_h = 0.25$, in the disk fraction, defect density plane. ρ_d acquires constant values at the solid-hexatic and hexatic-liquid boundaries.

The pentagon's discontinuous melting scenario extends over a large part of the diagram: melting becomes discontinuous as soon as the pentagon's fraction overcomes $f_h \simeq 0.25$. The KTHNY scenario always separates the mixed and discontinuous transitions regardless of the hexagon fraction.

In bidisperse systems, the defects' density controls the stability of the solid and hexatic phases. We have found the same occurs in the ternary mixtures. To demonstrate this, we focus here on ternary mixtures with a fixed fraction of hexagons, $f_h = 0.25$, and report analogs' results for other f_h values in the SM [29]. For the studied fraction of disks, $f_d \leq 1 - f_h$, we plot in Fig. 3(b) the value of ρ_d at the boundaries between the different phases the system traverses as the area fraction increases. Regardless of the f_d values, the solid and hexatic phases become unstable at $\rho_{d,s} \simeq 0.046$ and $\rho_{d,h} \simeq 0.123$, respectively, as observed in the binary mixtures and the pure phases.

We have studied the two-dimensional melting of mixtures of similar-sized hard disks, hexagons, and pentagons. The size similarity suppresses geometric frustration and ensures crystallization in the triangular lattice for all compositions. As such, changes in the relative composition allow us to investigate the interplay between the discontinuous melting scenario of hard pentagons, the mixed scenario of hard disks, and the KTHNY scenario of hard hexagons. Hexagons + disks mixtures smoothly cross over from the KTHNY to the mixed melting scenario; similarly, hexagons + pentagons mixtures cross over from the KTHNY to the discontinuous melting scenario. On the contrary, in disks + pentagons mixtures, the KTHNY melting may result from the competition between hard disks' mixed melting scenario and pentagons' discontinuous one: two dogs strive for a bone, and the third runs away with it. The exhaustive investigation of the melting of two- and three-component mixtures further corroborates speculated [22] melting criteria and establishes new ones based on the density of defects. The solid phase becomes unstable for $\rho_d > \rho_{d,s}$, the hexatic phase for $\rho_d > \rho_{d,h}$. The connection of these criteria with previously speculated Lindemann-like ones [25–27] and the possibility of relating the free energy of the phases to the defect's density are fascinating future research directions that could lead to a better understanding of the mechanisms driving the different melting pathways.

Y.-W. L. acknowledges support of the start-up funding of Beijing Institute of Technology and support from the National Natural Science Foundation (NSF) of China (Grants No. 12105012). Y. Y. is supported by the NSF of China (Grants No. 11734003, No. 12061131002). M. P. C. acknowledges support by the Ministry of Education, Singapore, under its Academic Research Fund Tier 2 (MOE-T2EP50221-0016) and Tier 1 (MOE-T1-RG56/21).

*yanweili@bit.edu.cn
†ygyao@bit.edu.cn
‡massimo@ntu.edu.sg

[1] J. M. Kosterlitz and D. J. Thouless, J. Phys. C **6**, 1181 (1973).
[2] B. I. Halperin and D. R. Nelson, Phys. Rev. Lett. **41**, 121 (1978).
[3] A. P. Young, Phys. Rev. B **19**, 1855 (1979).
[4] W. F. Brinkman, D. S. Fisher, and D. E. Moncton, Science **217**, 693 (1982).
[5] P. A. Heiney, P. W. Stephens, R. J. Birgeneau, P. M. Horn, and D. E. Moncton, Phys. Rev. B **28**, 6416 (1983).
[6] K. J. Strandburg, Rev. Mod. Phys. **60**, 161 (1988).
[7] J. A. Barker, D. Henderson, and F. F. Abraham, Physica (Amsterdam) **106A**, 226 (1981).
[8] E. P. Bernard and W. Krauth, Phys. Rev. Lett. **107**, 155704 (2011).
[9] A. L. Thorneywork, J. L. Abbott, D. G. A. L. Aarts, and R. P. A. Dullens, Phys. Rev. Lett. **118**, 158001 (2017).
[10] Y.-W. Li and M. P. Ciamarra, Phys. Rev. Lett. **124**, 218002 (2020).
[11] Y. Komatsu and H. Tanaka, Phys. Rev. X **5**, 031025 (2015).
[12] Y.-W. Li and M. Pica Ciamarra, Phys. Rev. Mater. **2**, 045602 (2018).
[13] S. Deutschländer, T. Horn, H. Löwen, G. Maret, and P. Keim, Phys. Rev. Lett. **111**, 098301 (2013).
[14] J. Downs, N. Smith, K. Mandadapu, J. P. Garrahan, and M. I. Smith, Phys. Rev. Lett. **127**, 268002 (2021).
[15] S. Deutschländer, A. M. Puertas, G. Maret, and P. Keim, Phys. Rev. Lett. **113**, 127801 (2014).
[16] D. Abutbul and D. Podolsky, Phys. Rev. Lett. **128**, 255501 (2022).
[17] S. C. Kapfer and W. Krauth, Phys. Rev. Lett. **114**, 035702 (2015).
[18] J. A. Anderson, J. Antonaglia, J. A. Millan, M. Engel, and S. C. Glotzer, Phys. Rev. X **7**, 021001 (2017).
[19] S. Prestipino, F. Saija, and P. V. Giaquinta, Phys. Rev. Lett. **106**, 235701 (2011).
[20] M. Zu, J. Liu, H. Tong, and N. Xu, Phys. Rev. Lett. **117**, 085702 (2016).
[21] J. Russo and N. B. Wilding, Phys. Rev. Lett. **119**, 115702 (2017).
[22] J. Guo, Y. Nie, and N. Xu, Soft Matter **17**, 3397 (2021).
[23] P. Sampedro Ruiz, Q.-l. Lei, and R. Ni, Commun. Phys. **2**, 70 (2019).
[24] P. Digregorio, D. Levis, L. F. Cugliandolo, G. Gonnella, and I. Pagonabarraga, Soft Matter **18**, 566 (2022).
[25] K. Zahn and G. Maret, Phys. Rev. Lett. **85**, 3656 (2000).
[26] S. A. Khrapak, Phys. Rev. Res. **2**, 012040(R) (2020).
[27] P. Dillmann, G. Maret, and P. Keim, J. Phys. Condens. Matter **24**, 464118 (2012).
[28] Y. Zong and K. Zhao, Curr. Opin. Solid State Mater. Sci. **26**, 101022 (2022).
[29] See Supplemental Material at http://link.aps.org/supplemental/10.1103/PhysRevLett.130.258202 for additional information about numerical details, thermal equilibration, finite size effects, temperature dependence of the melting, the melting of bidisperse and ternary systems, and defects.
[30] J. D. Weeks, D. Chandler, and H. C. Andersen, J. Chem. Phys. **54**, 5237 (1971).
[31] Y. Zhu, H. Liu, Z. Li, H. Qian, G. Milano, and Z. Lu, J. Comput. Chem. **34**, 2197 (2013).
[32] C. N. Likos and C. L. Henley, Philos. Mag. B **68**, 85 (1993).
[33] O. Uche, F. Stillinger, and S. Torquato, Physica (Amsterdam) **342A**, 428 (2004).
[34] J. A. Perera-Burgos, J. M. Méndez-Alcaraz, G. Pérez-Ángel, and R. Castañeda-Priego, J. Chem. Phys. **145**, 104905 (2016).
[35] E. Fayen, A. Jagannathan, G. Foffi, and F. Smallenburg, J. Chem. Phys. **152**, 204901 (2020).
[36] B. P. Prajwal and F. A. Escobedo, Phys. Rev. Mater. **5**, 024003 (2021).
[37] R. J. Speedy, J. Chem. Phys. **110**, 4559 (1999).
[38] J. E. Mayer and W. W. Wood, J. Chem. Phys. **42**, 4268 (1965).
[39] We associate to each particle a local density defined as $\phi_{\mathrm{loc}}(\vec{r}_i) = [\sum_{j=1}^{N} A_j H(r_c - |\vec{r}_i - \vec{r}_j|)/\pi r_c^2]$, where A_j is the area of particle j, H is the Heaviside step function, and $r_c = 21d$.
[40] Y.-W. Li and M. P. Ciamarra, Phys. Rev. E **100**, 062606 (2019).
[41] N. D. Mermin and H. Wagner, Phys. Rev. Lett. **17**, 1133 (1966).
[42] A. Toyotama, T. Okuzono, and J. Yamanaka, Sci. Rep. **6**, 23292 (2016).